



N-INNER Program 2008-2011

Scientific Report April 2012

Background and Objective

Solar Hydrogen was a joint effort of four scientific groups representing Chalmers University, University of Oslo, Technical University of Denmark and University of Iceland with the overall aim to develop new electrode materials and schemes for photocatalytic water splitting for hydrogen production and contribute to the overall understanding of the fundamental processes of photocatalytic water dissociation. The projects program was evaluated and recommended in 2008 as one of the five so-called “N-INNER – 1” projects. The project was financed by the national energy agencies of the participating partners. Professor Dinko Chakarov from the Department of Applied Physics, Chalmers University, coordinated the project.

More specifically, the partners work separately and in collaboration in the following areas:

- * Nanofabrication and plasmon coupled photon energy transfer (Chalmers University of Technology).
- * Corrected/Extended DFT applied to studies of excitations and charge carriers (University of Island).
- * Identification/characterization of novel oxide materials and their band gap engineering. (Univ. of Oslo)
- * Materials preparation and characterization; Instrument development, new photo reactors with MEMS technology. (Danish Technical University).

Thus, the objective was to acquire a detailed understanding of the mechanisms behind water photodissociation with solar light using both experiment and theory. Specific for the approach was to scrutinize the potential of nanoscience and nanotechnology in the above context of water-splitting devices with improved efficiencies and durability.

The description below covers the scientific results of the project. All organizational details (participants, networking, organization, cooperation etc. are reported through the annual administrative reports to N-INNER; the financial issues are reported to the respective financing organizations of the respective partners.

Introduction

Photo-electrochemical (PEC) water splitting into hydrogen and oxygen on semiconductor/electrolyte interface is a very attractive approach to develop the sustainable energy systems, which can meet the increasing energy demand mainly relying on the fossil-fuel currently. The key is to find the semiconductor materials for stable and cost-effective PEC hydrogen production system. Secure and abundant energy supply is one of the most important challenges for the global society. Hydrogen is the preferable *base* of an environmentally acceptable energy system, which will be able to eventually replace the fossil fuels on a time scale of 20-50 years (for reviews on Hydrogen Economy and its “dead”, see e.g. [1, 2]). This is because of its advantages for use in mobile applications, energy storage and electrical net load balancing. There is a consensus in literature that the most promising method of hydrogen generation using a renewable energy source is that based on solar photo electrochemical (PEC) water decomposition [3]. In principle, visible light has enough energy to split H₂O into hydrogen and oxygen. However, water is transparent in the visible and doesn't absorb this energy. The combination of a light harvesting system and a H₂O splitting system is thus necessary. In spite of the fact that PEC water splitting was demonstrated long ago [4], and the general requirements for solar photonic converters have been well defined [5], current methods and devices are still inefficient, and consequently the price of solar hydrogen is too high for the technology to enter a significant market. This is due to several weaknesses of the current systems: limited absorption in the visible, where the solar irradiation has the highest power density at the Earth surface; fast electron-hole (e-h)

recombination and fast back-reaction of H and O to form H₂O again; and difficulties of matching the semiconductor band-edge energies with the H₂ and O₂ evolution reactions. Another problem is the corrosion resistivity of the electrodes - the most efficient semiconductors are unstable upon irradiation in water. One can conclude that the energy conversion efficiency of PEC water splitting is determined to a great extent by the properties of the materials used for photo-electrodes. Consequently, commercial applications for hydrogen generation from solar energy and water will be determined by the progress in materials science and engineering applied to the materials for photo-electrodes. Additionally, the emerging field of nanoscience and nanotechnology has great potential to contribute to improved water splitting devices via various pathways. Therefore this project was directed to identify proficient light utilization schemes, lower cost materials, and systems that are efficient, durable and stable.

The objective of our work was to discover and characterize the candidate electrode materials and understand specific elements of their performance. Basically, these materials should be functioned as: (1) light absorber to generate electron and hole upon illumination; (2) junction formed on the semiconductor/electrolyte interface to separate the photo-generated carriers; (3) electro-catalyst for the gas evolution (either oxygen for n-type semiconductor or hydrogen for p-type semiconductor) to improve the kinetics of the electrode reaction. Additionally, the candidate materials should have high stability and abundant.

Results

The general approach of this project was to integrate synthesis, characterization, test and theory to identify and develop the promising materials to meet the PEC challenge in efficiency, stability and cost. Various synthesis techniques were used to tailor the surface structure of the materials. Their micro-structural, electrochemical and photo-electrochemical characterizations were investigated in detail. Within this project, we focus on the materials which are regarded as interesting candidates for PEC application. These materials include TiO₂-based (pure and composites with e.g. carbon), band gap engineered ZnCdO absorbers, Fe₂O₃-based photo-anodes and Si-based photo-cathodes.

1. Fabrication

For the fabrication we used state-of-the-art experimental approaches applying nanotechnology, including advanced facilities at MC2 (Chalmers), MEMS facility "DANCHIP at DTU" and MinaLab (UiO). The main method at the UiO was magnetron-sputtering and MOCVD for the preparation of metal oxide based thin films. Examples are the graded Zn-Cd oxide samples, schematically shown on Figure 1. The idea is to prepare stacks of layers with stepwise increasing bandgap for the purposes of efficient light absorption over a broader part of the solar spectrum.

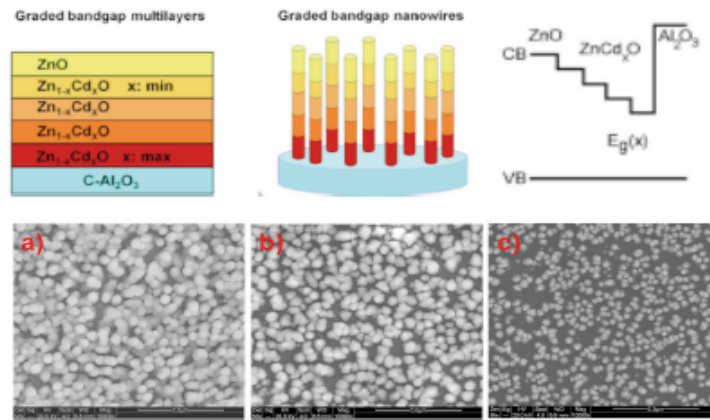


Figure 1. Schematic presentation and micrographs of the model samples prepared by magnetron-sputtering and MOCVD by Oslo group.

Nanofabrication methods at Chalmers include physical vapor deposition of the photocatalysts (TiO_2 and carbon) and hole-mask colloidal lithography for preparation of nanoplasmonic particles. Examples of prepared samples and their structure are shown on Figures 2 and 3.

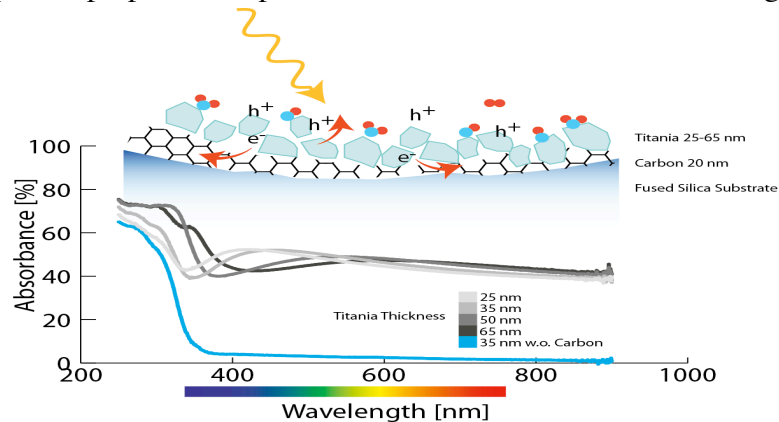


Figure 2. Optical absorption of TiO_2/C composite films of different thicknesses compared to 35 nm thick pure titania film prepared and investigated by Chalmers group.

The biggest advantage of the developed PVD method is the purity of prepared films and reproducibility of their structure and morphology (to be articulated below).

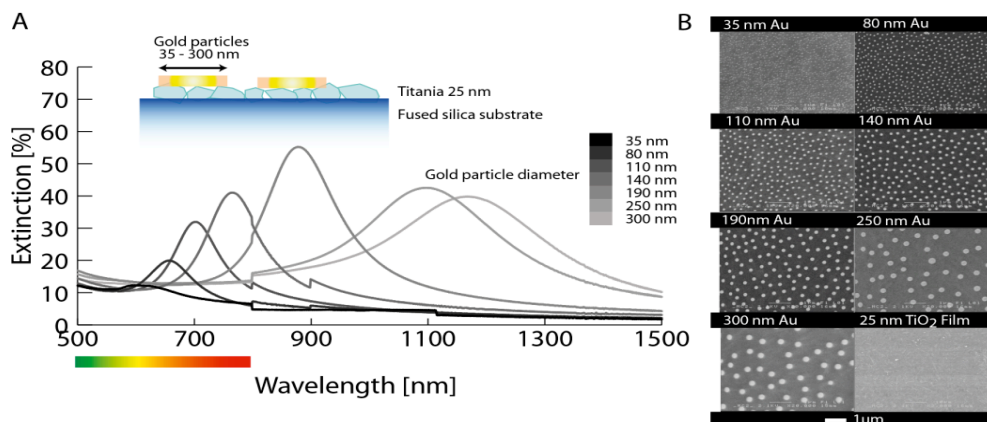


Figure 3. Optical extinction spectra for gold nanoparticles with different diameters on a titania thin film prepared by Chalmers group. Inset is a schematic of the prepared nanoparticle photocatalysts. B) SEM image of prepared films and their schematic composition.

Although it has wide band-gap, pure TiO_2 is still an interesting material for PEC water splitting due to its low-cost and high stability in the electrolyte. The TiO_2 nanotube arrays have received considerable attentions because of their high surface area and excellent charge transfer properties. Herein, highly ordered TiO_2 nanotubes were synthesized by electrochemical anodization of titanium foil in the ethylene glycol/fluoride electrolyte. Figure 4 shows the field emission scanning electron microscope (FESEM) images of a titanium oxide layer grown on Ti foil by anodization. It revealed that the layer contains pores that were parallel to each other and perpendicular to the substrate, the nanotubes were smooth, compact and robust.

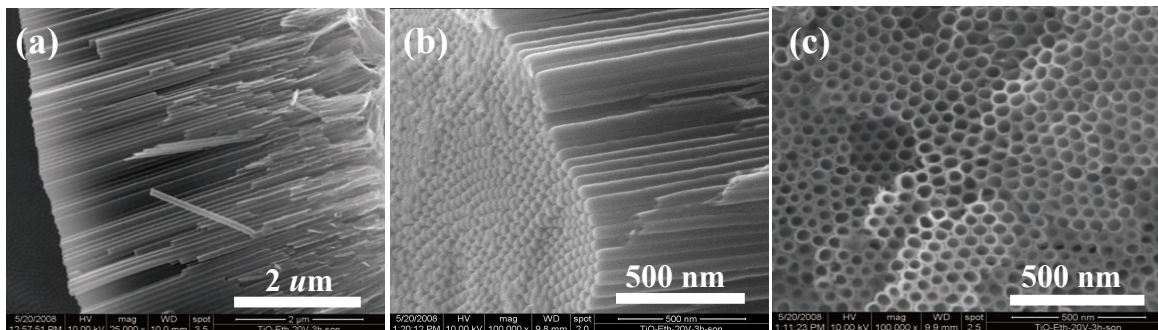


Figure 4. FESEM images of a TiO_2 nanotube array sample grown at 20 V in an ethylene glycol/fluoride electrolyte: (a) side view, (b) bottom view, (c) top view. Samples prepared and characterized by DTU group.

Analytical methods

At DTU we have developed systems for optical, electrochemical, and photo-electrochemical (irradiance spectrum, photocurrent, incident photon conversion to electrons) characterization, combined with gas chromatogram for quantitative H₂ and O₂ analysis, which is shown in **Figure 5**. The approach at Chalmers University was to combine the catalytic performance tests of the samples with mass spectrometry, Figure 6.

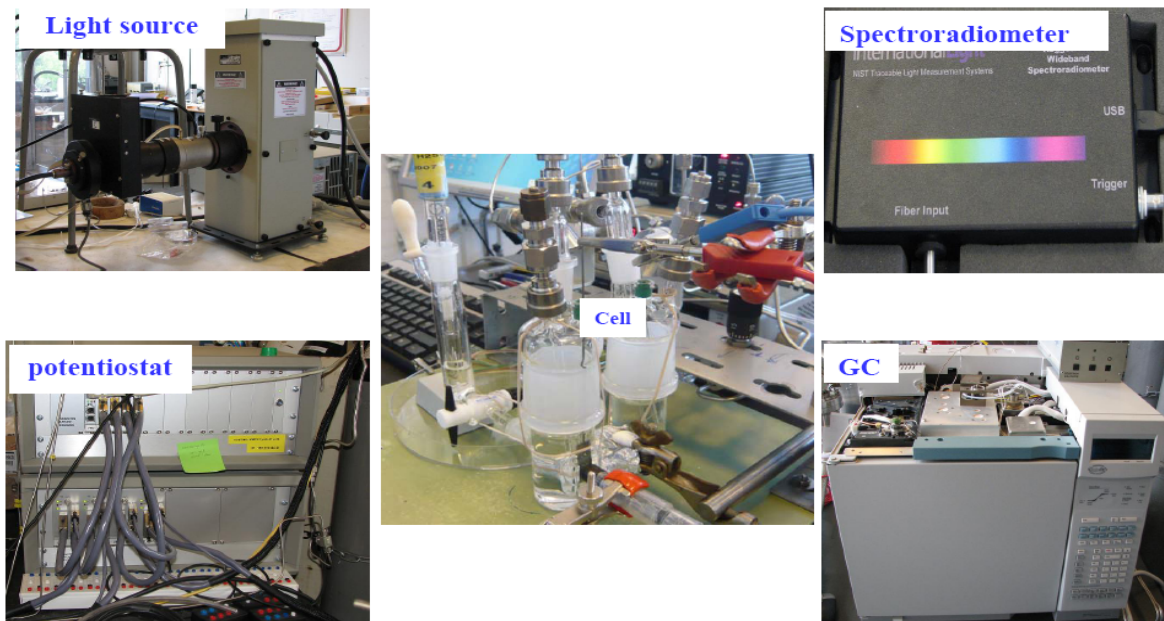


Figure 5. Photoelectrochemical water splitting systems developed at DTU.

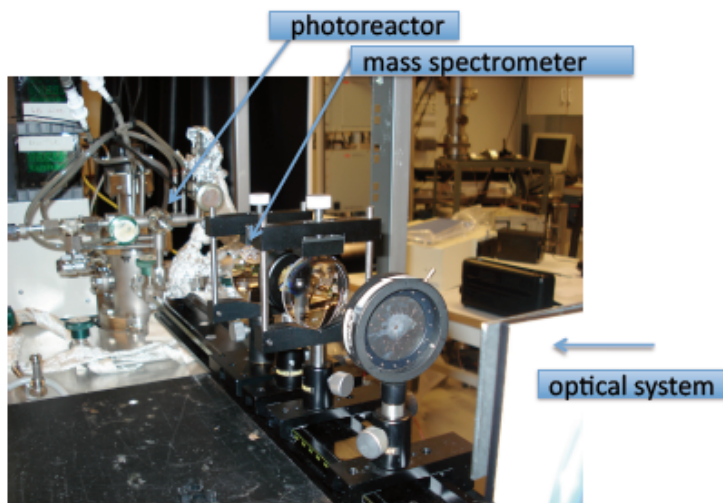


Figure 6. The experimental setup for photocatalytic measurements developed and used at Chalmers. It makes possible to monitor the products and intermediates of the photoreaction in real time.

These classes of the materials were investigated for PEC water splitting, the detailed progresses in developing these materials are in the following sections

Results:

TiO₂-based materials

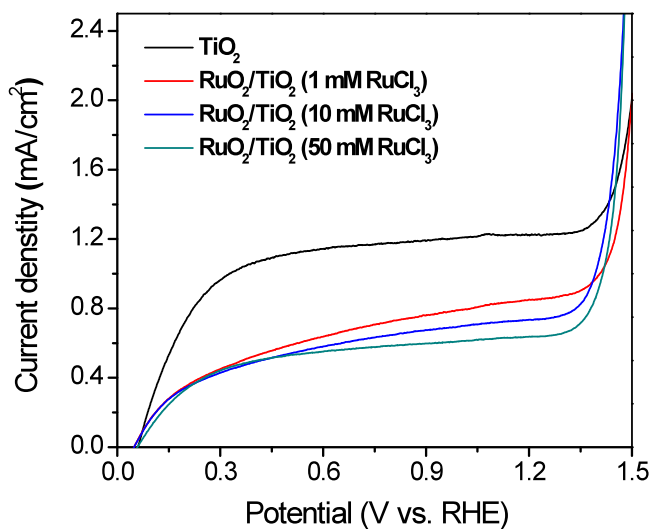


Figure 7. The variation of photocurrent density versus the potential for RuO₂/TiO₂ under UV light irradiation (290-390 nm, 75 mW/cm²), with TiO₂ as a reference.

We used RuO₂ as an oxygen evolution catalyst to improve the kinetics of water splitting over TiO₂ nanotube photoanode. The wet impregnation method was used to load the RuO₂. The variation of photocurrent density versus the potential for the samples was shown in Figure 7. The introduction of RuO₂ in TiO₂ nanotubes decreased the photocurrent of TiO₂ nanotubes. The more RuO₂ was introduced into the TiO₂ nanotube, the lower photocurrent the sample exhibited. This might be resulted in that the RuO₂ was the recombination centers of photo-generated carriers.

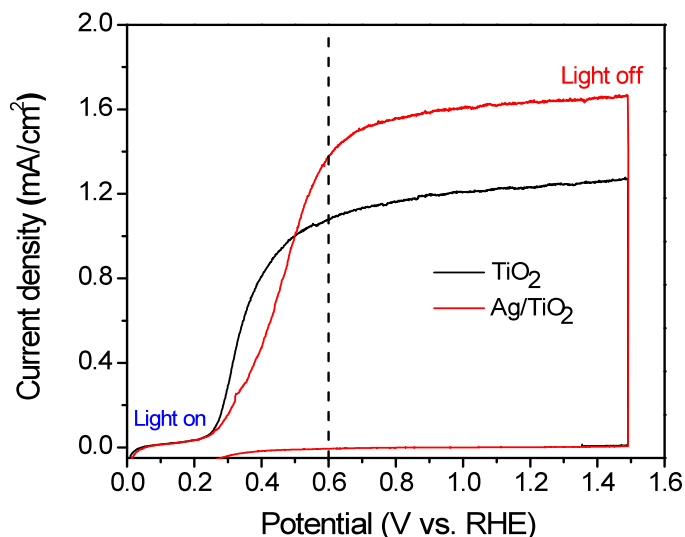


Figure 8. The variation of photocurrent density versus the potential for Ag/TiO₂ under UV light irradiation (290-390 nm, 75 mW/cm²), with TiO₂ as a reference.

We also investigate the effect of metal nanoparticles deposition on the performance of TiO₂ nanotubes. Here, the Ag nanoparticles were photodeposited onto the TiO₂ nanotubes. The variation of photocurrent density versus the potential was presented in Figure 8. For comparison, the performance of TiO₂ nanotubes was included. In comparison to the naked TiO₂ tubes, the photocurrent is improved by 30% over Ag/TiO₂ nanotubes at the potential of 0.6 V (vs. RHE). The stability experiments were run for 4 h under continued irradiation at the potential of 0.6 V (vs. RHE), no obvious photocurrent decay for the samples was observed in Figure 9. Simultaneously, the amounts of evolved H₂ and O₂ were measured by Gas chromatogram. The volume ratio of the evolved H₂ and O₂ was 2:1. The experimental measurement was in agreement with the calculation for H₂ evolution estimated by the integration of current-time curve, the results were shown in Figure 10. The conclusion is that the deposition of Ag nanoparticles can improve the PEC performance to some extent. However, its efficiency still very low, it only works under UV light and with imposed bias. In the future work, it is worth of investigating the couple TiO₂ nanotubes with low band gap semiconductors or doping TiO₂ with hetero-elements for utilization of visible light. Simultaneously, the efficient oxygen catalyst is needed to modify the TiO₂ and thus make it work under low bias or no bias.

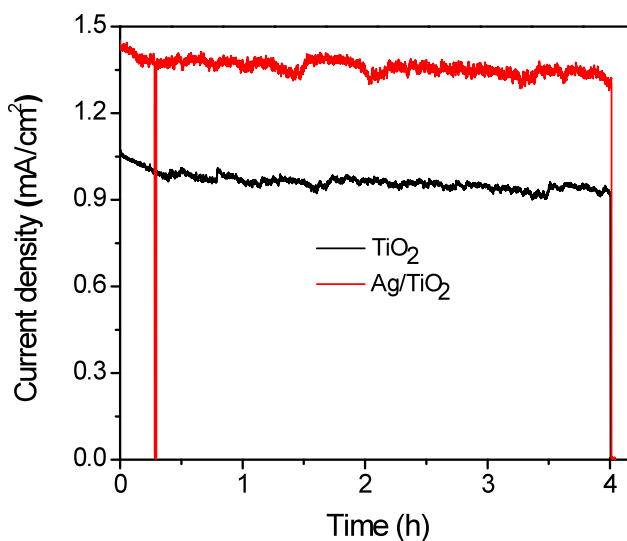


Figure 9 The potentiostatic plot showing photocurrent density recorded at the potential of 0.6 V (vs. RHE) for 4h under UV light irradiation (290-390 nm, 75 mW/cm²).

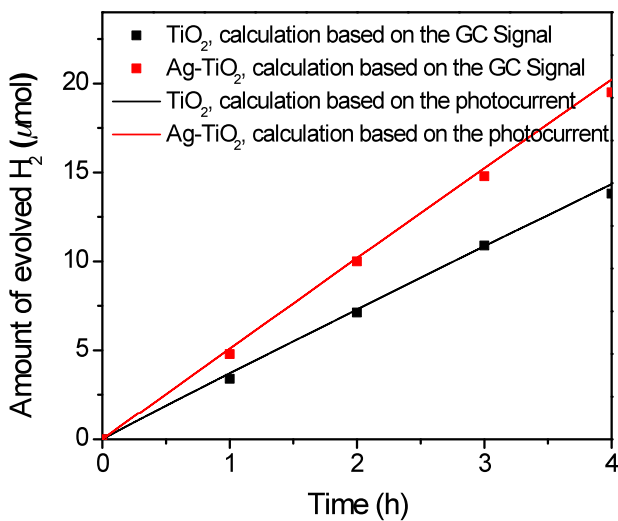


Figure 10 Time course of H₂ evolution from the TiO₂ and Ag/TiO₂ photoelectrodes.

Additionally, the TiO₂ nanotubes grown on non-conductive substrate (pyrex glass) were developed and used for decomposition of volatile organic compounds (such as acetone). Figure 11 shows that the TiO₂ nanotubes film has better performance than commercial P25

film. This can be applied in the treatment of air pollution indoors using photocatalysis technology.

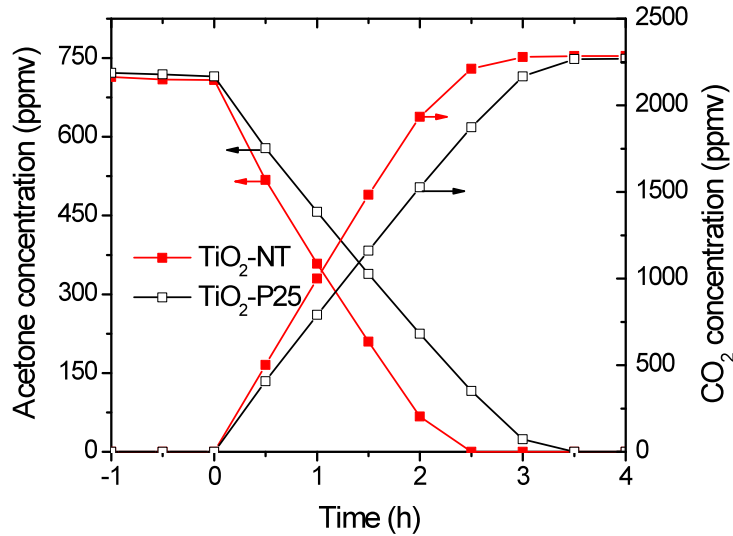


Figure 11. Changes in acetone (left axis) and CO₂ concentrations (right axis) are plotted as a function of time in the presence of a TiO₂ NT-array film (red lines, filled boxes) and a P25 thin film (black line, open boxes) under UV irradiation.

We work with TiO₂ deposited on graphitic-like carbon film as shown in Figure 2. Additionally to the enhanced absorption in the visible, the carbon film promotes efficient separation of photogenerated charge carriers because of its anisotropic conductivity for electrons and holes. As the photoreaction occurs on the surface of the TiO₂ catalyst, it is of great interest to investigate thickness dependence of charge transport in the titania films and how the presence of carbon film affects the size of crystallites. Both carbon and titania films were prepared by e-beam evaporation and DC reactive magnetron sputtering, respectively, at room temperature on a fused silica substrate. Postdeposition annealing was carried out to reduce internal stresses and improve crystallinity in the film at 800°C and 500°C for carbon and TiO₂, respectively. Optical measurements of the composite films with different thicknesses are illustrated in Figure 12. The general observation is that composite films absorb more in the visible than pure titania films. Most importantly, the absorption threshold of TiO₂ has red shifted for composite films.

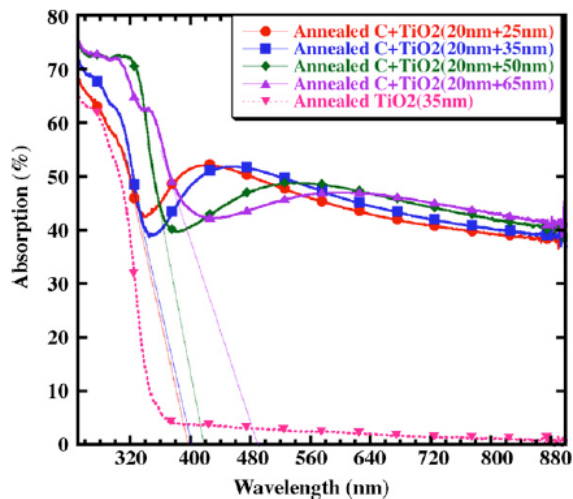


Figure 12. Optical absorption of composite films with different thicknesses of TiO₂ deposited on fused silica. Absorption edge has been marked by a tangent line for all spectra.

The catalytic activity of the films was tested in the reaction of photo-oxidation of methanol to CO₂ and water. The measurements were made in a, for this purpose constructed, minireactor (~880 μ L volume, see Figure 6) in batch mode under UV light illumination of 120mW/cm². The products were monitored in situ by a mass spectrometer coupled to the reactor via a capillary. The rates of CO₂ formation as a function of photocatalysts composition were obtained by monitoring $m/z = 44$ mass spectrometer signal and are summarized in Figure 13. Accordingly, composite films clearly have enhanced photoactivity compared to pure titania films. The observed enhancement of photocatalytic activity is assigned to synergy effects at the carbon/TiO₂ interface, resulting in smaller titania crystallites and anisotropic charge carrier transport, which in turn reduces their recombination probability. Variation in photoactivity with the thickness of the titania layer, both for pure and composite films, can be seen from the figure. The activity gradually increases up to certain thickness after which it starts to decrease. Once the film thickness reaches optimum value (~mean free path distance), it encounters more scattering on its way to the surface. As a consequence, the photoactivity decreases at thicknesses beyond the optimum due to enhanced trapping of charge carriers although the optical absorption volume of the films increases. Overall, this measurement clearly discriminates the effect of thickness on charge transport and photoactivity as discussed above.

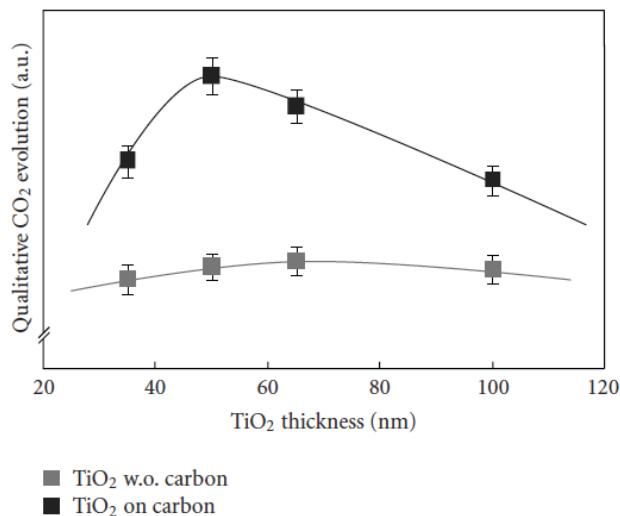


Figure 13. CO₂ formation as result of photocatalytic oxidation of methanol under UV illumination. The results for composite films (dark data points) are compared with these for pure titania films (light data points) at several thickness. The solid lines are guides for the eye.

Further, in the search for the origin of the enhanced photocatalytic activity of composite TiO₂-carbon systems, we fabricated and analyzed well-defined model samples consisting of anatase and graphitic carbon with and without modifying the interface between them by a thin SiO₂ space layer (Figure 14). The films with a TiO₂/C interface show noticeably lower photoluminescence intensity and shorter carrier life times compared to single TiO₂ films with the same thickness and composition. The stronger non-radiative recombination is mainly assigned to charge carrier leakage (transfer) at the interface between TiO₂ nanocrystallites and the carbon film. Figure 15 illustrates the discussed mechanism.

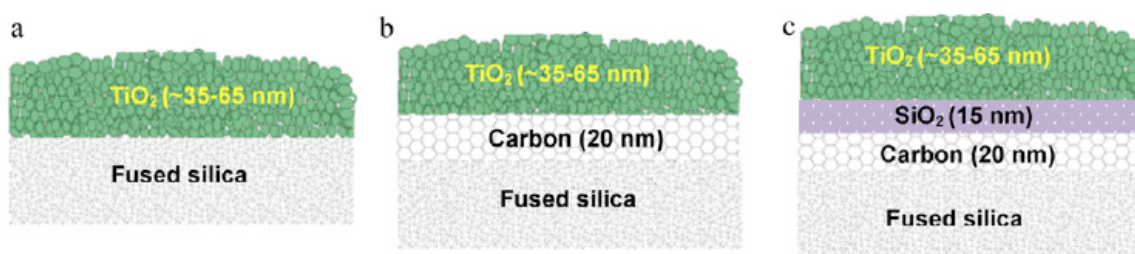


Figure 14. Schematic of three different composition of fabricated samples: (a) single TiO₂ films with different thicknesses (~35 to ~65 nm); (b) composite films consisting of a 20 nm thick carbon and different thicknesses of TiO₂ films as in (a); and (c) sandwiched thin SiO₂ (~15 nm) layer in between the carbon and TiO₂ films as in (b). The size of the TiO₂ crystallites vary depending on the sample composition and is in the range of ~20 nm to ~30 nm. The crystallite size was estimated using the Scherrer equation and (1 0 1) peak obtained from the XRD spectra (not shown).

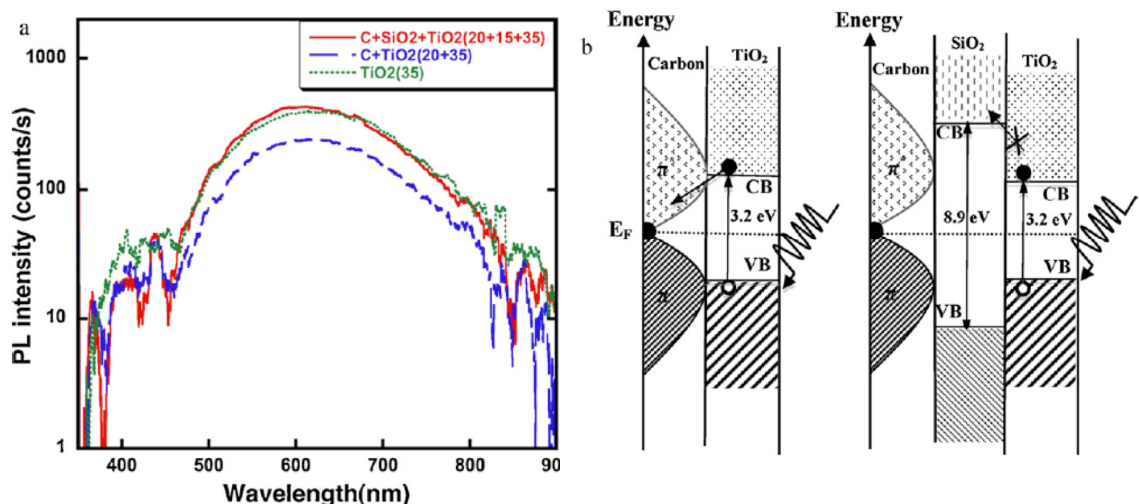


Figure 15. PL spectra of composite films samples with and without a 15 nm spacer SiO₂ layer in between the carbon and TiO₂ films (note the logarithmic scale). (b) Energy band diagram corresponding to the respective sample structures. The band diagram of carbon corresponds to graphite. Note the low but finite electron density in graphite at the Fermi level. Note also the high-energy barrier for photogenerated electrons in the presence of space layer in contrast to the situation with direct TiO₂/C contact.

Fe₂O₃-based materials

Fe₂O₃ has a band gap of 2.1 eV, it means that it can utilize visible light. Furthermore, its valence band edge energy is suitable for water oxidation, and it is also abundant and stable in most electrolytes. Unfortunately, the poor conductivity of Fe₂O₃ thin films limits their practical applications. Recently, Gratzel et al reported that Si-doped porous films synthesized by atmospheric pressure chemical vapor deposition (APCVD) showed an exceptionally high photo-current of 2.3 mA/cm² at 1.23 V (vs. RHE) under the simulated AM1.5 sunlight. We also used the APCVD method to prepare the Si-doped Fe₂O₃. Figure 16 shows the typical SEM image of the as-prepared film, the film consists of the dendritic structures with more finely divided branches, similar to the reported. Figure 17 shows the current-potential curves for a Si-doped Fe₂O₃ electrode in the dark and under irradiation. The dark current is negligible up to about 1.6 V (vs. RHE). The photocurrent densities with the front-side irradiation are higher than those with back-side irradiation. This is attributable to the larger surface area of the film surface. In Figure 17b, we can see that the photocurrent density with the front-side irradiation is about 2.0 mA/cm² at the potential of 1.23 V (vs. RHE) even under visible light irradiation. However, a high bias is needed in this system. Future efforts will

focus on the search of cheap electrocatalytic oxygen evolution catalyst to decrease the bias or tuning the conduction band edge position of Fe_2O_3 .

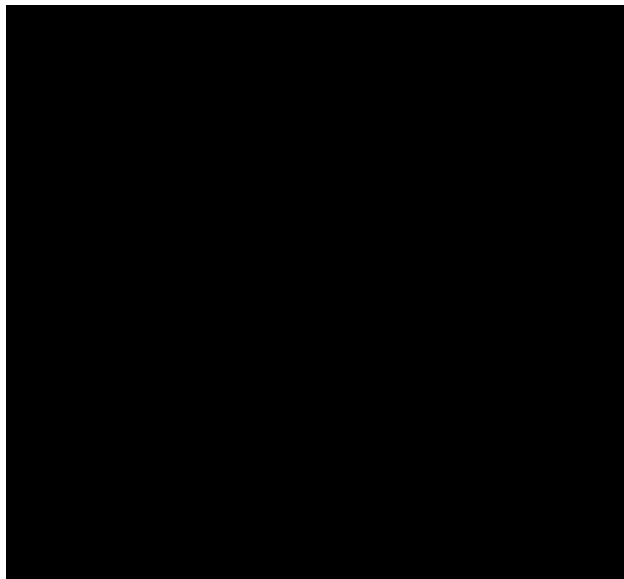


Figure 16 SEM images of Fe_2O_3 films grown by APCVD on FTO conducting glass

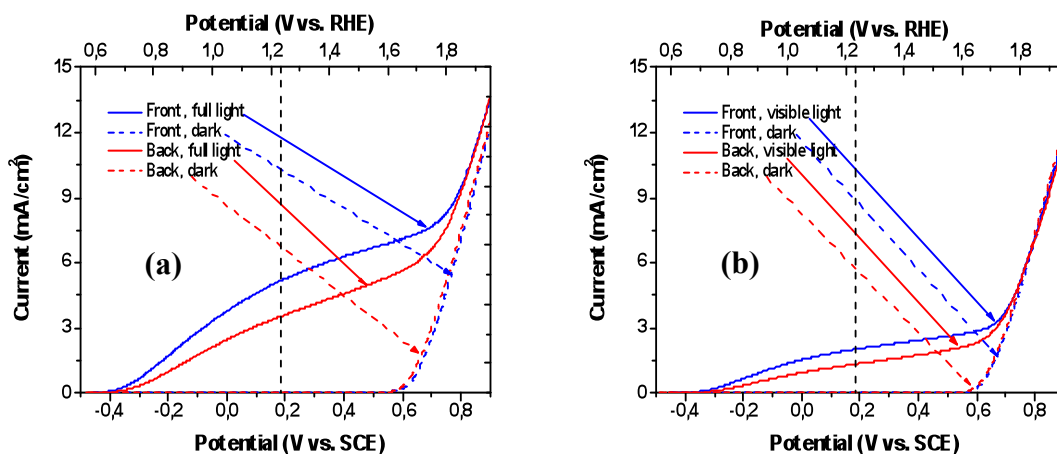


Figure 17. Dark (dashed) and photocurrent (solid) densities for a Si-doped Fe_2O_3 photocathode under 150 W Xenon light source irradiation through front (blue) and back (red) side, with the front side being defined as the electrolyte/semiconductor interface: (a) without filter and (b) with cut-off filter ($\lambda > 420$ nm)

Si-based materials

So far, no appropriate material for a single-photon system for water splitting has yet been discovered. By combining a small band gap and a large band gap semiconductor, the two-

photon tandem approach allows access to a larger part of the solar spectrum than single-photon water splitting, and potentially has a higher solar to hydrogen efficiency. When considering photocathode materials, silicon (Si) is an interesting candidate as a light absorber due to the low band gap (1.1 eV), the low band gap enables effective utilization of the visible and IR light from the sun. However, Si alone has rather poor hydrogen evolution kinetics. It is therefore required to catalyze the hydrogen evolution by loading an electro-catalyst onto the Si surface. Here we developed molecular cluster HER catalyst to activate the *p*-Si toward hydrogen evolution upon illumination. Seen in Figure 18a, under illumination the naked planar Si has an onset of photo current at $U_{\text{RHE}} = -0.4$ V. Upon depositing the Mo_3S_4 clusters a significant enhancement in photocurrent is observed, with an onset shifted to $U_{\text{RHE}} = +0.15$ V due to improved catalysis. This results in a hydrogen evolution current density of 8 mA/cm^2 at the reversible potential ($U_{\text{RHE}} = 0$ V). In order to further improve the photo-electrochemical activity of this system. We prepared Si pillars with high aspect ratios using a photo-lithographic method. Scanning electron micrograph characterization of the pillars is shown in Figure 18b. The resulting Si pillars are completely oriented and highly regular, with the diameter of 3 μm and the height of 50 μm . The photo-electrochemical data in Figure 18a shows that the naked Si pillars are considerably improved relative to planar Si, the limiting current density of the pillar electrode is about 16 mA/cm^2 corresponding to an IPCE of 93%, 33% higher than that of the planar Si. The photo-activity was further improved by depositing Mo_3S_4 cluster catalyst onto the Si pillar electrode, yielding a sample that reaches 9 mA/cm^2 at $U_{\text{RHE}} = 0$ V. The current densities at the reversible potential match the requirement of a photoelectrochemical hydrogen production system with a solar-to-hydrogen efficiency in excess of 10%.

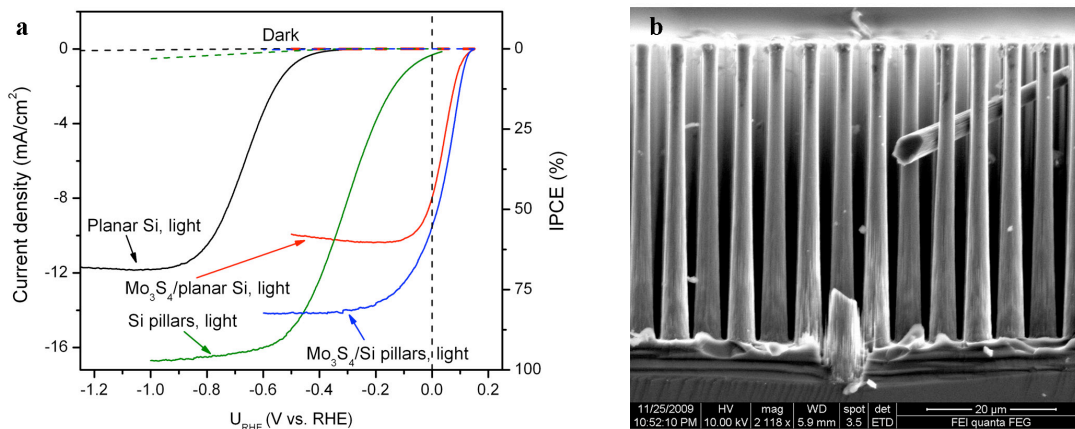


Figure 18. (a) The potentiodynamics runs on the photoelectrodes. Steady-state current density-voltage (left axis) is run in aqueous 1.0 mol/L HClO₄ solution under red light irradiation ($\lambda > 620$ nm, 28.3 mW/cm²) and the calculated incident photon-to-current conversion (IPCE) is shown on the right axis. The almost horizontal dashed lines denote the current measured in darkness (almost zero mA/cm²). (b) Scanning electron micrograph of Si pillars.

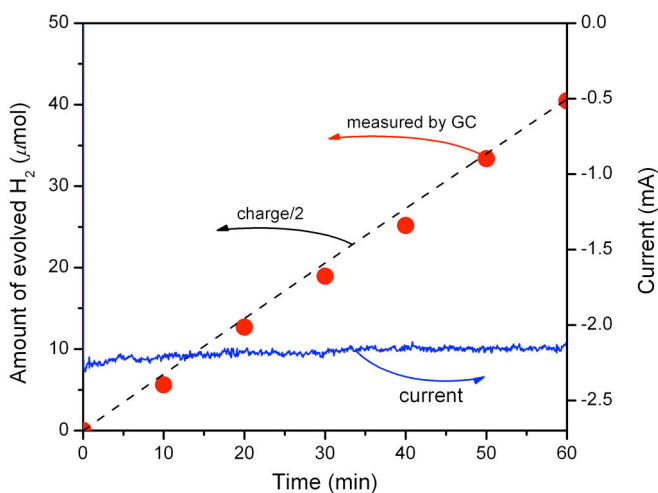


Figure 19. Stability of hydrogen evolution as a function of time measured with a gas chromatograph (left axis) and corresponding current (right axis) over Mo₃S₄/Si pillars at U_{RHE} = 0 V. The illuminated area is ~ 0.25 cm² and the sample is under red light irradiation ($\lambda > 620$ nm, 28.3 mW/cm²).

The stability of the Mo₃S₄/Si pillars electrode were run at U_{RHE} = 0 V under red light irradiation over 60 min. The electrode remains stable as shown by the blue line in *Figure 19*. Direct quantification of the H₂ was performed on the same Mo₃S₄/Si pillars electrode (shown as the red dots). The measured amount of H₂ closely matches half of the number of electrons

passed through the circuit (shown as the black dashed line). This demonstrates that the current is indeed due to photocatalytic hydrogen evolution with unity Faradayic efficiency, and not a reduction of the Mo_3S_4 cluster.

We also have investigated the influence of the cluster-core unit in cluster-decorated p-Si on the photo-electrochemical (PEC) hydrogen evolution by using the homologous series of cubane-like heterobimetallic sulfide compounds. These compounds stem from the clusters of A_3S_4 and A_3BS_4 ($\text{A}=\text{W}, \text{Mo}$; $\text{B}=\text{Co}, \text{Cu}$). We find that the Mo-based cluster-decorated Si photoelectrodes show higher PEC performance than W-based cluster-decorated ones. This is consistent with the electrocatalytic activity of the clusters supported on *n*-Si. The result of stability tests shows that A_3CoS_4 ($\text{A}=\text{W}, \text{Mo}$) cluster-decorated p-Si photoelectrodes are not stable upon illumination. Furthermore, We also performed a series of density functional theory calculations on a model system, the calculated ΔG_{H^*} of model cluster adsorbed on H-Si(100) supports the experimental observation over cluster/*n*-Si toward hydrogen evolution.

Theory

An algorithm for the implementation of an extension of density functional theory, the so-called self-interaction correction, was developed further to make it possible to study electronic defect states such as localized electrons and electron holes as well as the energy of photons that can be absorbed by a material (band gap). Without the self-interaction correction, the commonly used density functional theory calculations cannot be used to study electronic defect states (because of too large tendency to delocalize electronic states) and band gaps. The method was implemented in the GPAW software suite as well as in a program called QuantIce that has been developed in the group. Calculations of TiO₂ and ZnO were carried out and are still ongoing. An example of results obtained is the characterization of the defect state at an oxygen vacancy of a TiO₂ surface where two electrons in a triplet state were found to be localized. The formation energy of the vacancy as well as binding energy of various ad molecules was calculated. The energetics of doping of ZnO with Cd were also calculated, as well as the interaction of the dopants with defects, such as oxygen vacancies.

Conclusion and Future Directions

1. We developed the systems for optical, electrochemical, and photoelectrochemical (irradiance spectrum, photocurrent, incident photon conversion to electrons) characterization, combined with gas chromatogram for quantitative H₂ and O₂ analysis.
2. We synthesized various TiO₂-based materials (carbon composites, nanotubes photoanode by electrochemical anodization method) and found that the deposition of Ag can improve its photocurrent to some extent, but the introduction of oxygen evolution catalyst (RuO₂) kills its performance. Furthermore, the TiO₂ nanotubes grown on pyrex glass was developed and used for decomposition of volatile organic compounds non. Coupling TiO₂ nanotubes with low band gap semiconductors or doping TiO₂ with hetero-elements might make it utilize the large fraction of sunlight-visible light.
3. Nanostructured Si-doped Fe₂O₃ films were deposited by atmospheric pressure chemical vapor deposition. The preliminary result showed a promising performance for water photooxidation. The introduction of the cheap electrochemical oxygen catalysts or the tuning of valence band edge of the nanostructured Fe₂O₃-based film will decrease the overpotential of solar water splitting.
4. We developed the photocathodes by coupling the bio-inspired cubane-like clusters to *p*-Si for hydrogen evolution, and investigate the structure effect of the cluster on their photocathode. Under illumination with the red part of simulated sunlight, the current density reaches 8 mA/cm² at the reversible hydrogen evolution potential over Mo₃S₄/*p*-Si. Furthermore, clusters supported on Si pillars show an enhanced performance, which is promising for potential application in a “chemical solar cell”. The DFT calculations support the experimental observation. At present, the output efficiency of cluster/*p*-Si is still low, a better HER catalyst and *p*-Si semiconductor with more positive open circuit potential are still needed. Finally, the overall water splitting with high solar-to-hydrogen efficiency will be obtained by combination of the photocathode and the photoanode (e.g. Fe₂O₃).

References and publications

1. Jeremy Rifkin, THE HYDROGEN ECONOMY, Publisher: J. P. Tarcher; (2002) ISBN: 1585421936
2. <http://www.technologyreview.com/blog/energy/23506/>
3. Serpone N, Lawless D, Terzian R. Solar Fuels: Status and Perspectives. *Solar Energy* 1992;49:221–34.
4. A. Fujishima, K. Honda, *Nature* 238, p 37. 1972
5. Allen J. Bard & MaryeAnne Fox: Perspective “Holy Grails of Chemistry”, *Accounts of Chemical Research*, vol 28 (1995) “Artificial Photosynthesis: Solar Splitting of Water to Hydrogen and Oxygen”
6. Tuning light absorption by band gap engineering in ZnCdO as a function of MOVPE-synthesis conditions and annealing, V.Venkatachalapathy, A.Galeckas, R.Sellapan, D.Chakarov and A.Yu.Kuznetsov, *Journal of Crystal Growth*, 314, 301 (2011).
7. Understanding of phase separation in ZnCdO by combination of structural and optical analysis, V.Venkatachalapathy, M.Trunk, T.Zhang, A.Azarov, A.Galeckas and A.Yu. Kuznetsov, *Phys. Rev. B* 83, 125315 (2011).
8. Temperature dependence of surface plasmon mediated near band-edge emission from Ag/ZnO nanorods, Y. P. Liu, Y. Guo, J. Q. Li, M.Trunk, A. Yu. Kuznetsov, J. B. Xu, Z. X. Mei, and X. L. Du, *Journal of Optics* 13, 75003 (2011).
9. Testing ZnO based photoanodes for PEC applications, M.Trunk, A.Sobas, V.Venkatachalapathy, T.Zhang, A.Galeckas, A.Yu.Kuznetsov, *Energy Procedia*, accepted.
10. Mechanism of enhanced photocatalytic activity of composite TiO₂/carbon nanofilms, R.Sellappan, A.Galeckas, V.Venkatachalapathy, A.Yu.Kuznetsov, and D.Chakarov, *Applied Catalysis B: Environmental*, doi:10.1016/j.apcatb.2011.05.036
11. Cd diffusion and thermal stability of CdZnO/ZnO heterostructures, A.Yu. Azarov, T. Zhang, B.G. Svensson, and A.Yu. Kuznetsov, *Appl.Phys.Lett.*, **99**, 111903 (2011).
12. Surface/strain energy balance controlling preferred orientation of CdZnO film, T.C.Zhang and A.Yu.Kuznetsov, *J.Appl.Phys.*, accepted
13. Time-resolved spectroscopy of carrier dynamics in graded ZnCdO multilayered structures, M. Trunk, V. Venkatachalapathy, T.C. Zhang, A. Azarov, A. Galeckas, and A. Kuznetsov, *Appl.Phys.Lett.*, submitted
14. H. Jónsson, *Proceedings of the National Academy of Sciences* 108, 944 (2011).
15. P. J. Klupfel, S. Klupfel, K. Tsemekhman and H. Jónsson, *Lecture Notes in Computer Science* (in press).
16. S. Klupfel, P. J. Klupfel, and H. Jónsson, *Phys. Rev. A* (submitted).
17. A.Valdes, J.Brillet, M.Graetzel, H.A.Hansen, H.Jonsson, P.Klupfel, S.Klupfel, G.-J. Kroes, F. Le Formal, I.C. Man, R.S. Martins, J.K. Nørskov, J.Rossmeisl, K. Sivula and M. Zacher, *Energy & Environmental Science* (submitted, 2011).
18. S. In, Y. Hou, B. Abrams, P. C. K. Vesborg, and I. Chorkendorff, Controlled Directional Growth of TiO₂ Nanotubes Using Molecular Oxygen as a Catalyst, *J. Electrochem. Soc.* 157 (2010) E69-E74.
19. P. C. K. Vesborg, S. In, J. L. Olsen, T.R. Henriksen, B. L. Abrams, Y. Hou, A. Kleinman-Shwarscstein, O. Hansen and I. Chorkendorff, Quantitative measurement of

- photocatalytic CO-oxidation as a function of light intensity and wavelength over TiO₂ nanotube thin films in micro-reactors, *J. Phys.Chem.C* 114 (2010) 11162-11168.
20. S. In, M. G. Nielsen, P.C. K. Vesborg, Y. Hou, B. L. Abrams, T.R. Henriksen, O. Hansen, and I. Chorkendorff, "Photocatalytic methane decomposition over vertically aligned transparent TiO₂ nanotube arrays", *Chem. Commun.* 47 (2011) 2613–2615.
 21. Y. Hou, B. L. Abrams, P-C.K. Vesborg, M. E. Björketun, K.Herbst, L. Bech, A. M. Setti, C. D. Damsgaard, T.Pedersen, O. Hansen, J. Rossmesl, S.Dahl, J. K. Nørskov,, and I. Chorkendorff, "Bioinspired Co-catalysts Bonded to a Silicon Photocathode for Solar Hydrogen Evolution " *Nature Materials* 10 (2011) 434-438.
 22. Y. Hou, B. L. Abrams, P-C.K. Vesborg, M. E. Björketun, K.Herbst, L. Bech, T.Pedersen, O. Hansen, J. Rossmesl, S.Dahl, J. K. Nørskov,, and I. Chorkendorff, Photoelectrocatalysis and electrocatalysis on cubane-like cluster-decorated silicon electrodes (*in preparation*)
 23. S. In, P.C. K. Vesborg, B.L. Abrams, Y. Hou, and I. Chorkendorff., "Does nitrogen doping of TiO₂ nanotubes really enhance the visible light photooxidation of organics?", *Journal of Photochemistry and Photobiology A: Chemistry* 222 (2011) 258-262.
 24. B. L. Abrams, Y. Hou, P. C.K. Vesborg, S. In, C. Damsgaard, O. Hansen, K. Herbst, and I. Chorkendorff, "Materials for photoelectrocatalytic hydrogen production", *EPO Patent Application No.:10000303.7 and USA Provisional Patent Application No.: 61/294866 (2010).*

The project results were presented on number of conferences and invited seminars.